Design and Optimization of a Thermal Management Structure for EV-based Lithium-ion Battery Arrays

Lepeng Wang*, Yajie Jiang
School of Electrical and Electronic Engineering, Nanyang Technological University, Singapore
**Corresponding Author*

Abstract: A thermal structure was designed and optimized in this study to minimize the thermal interaction between individual batteries, thus mitigating temperature distribution gradients and potential hotspots. the proposed structure achieved a 35% reduction in the maximum inter-cell temperature difference and maintained every cell below 40℃ during a 4C discharge pulse, demonstrating its practical effectiveness for EV duty cycles.

Keywords: Thermal Management; Multi-Battery System; Temperature Differences

1. Introduction

Effective thermal management is of great significance for ensuring the safety, longevity, and performance of multi-battery systems. Based on [1], [2], and [3], this study proposes a thermal‐management structure that isolates individual batteries, limits inter-battery heat transfer, and suppresses temperature gradients and local hot spots.

Early electro-thermal studies are performed based on fully coupled and physics-based partial-differential-equation (PDE) frameworks. Through a series of MATLAB-based parametric sweeps, the optimized architecture presented here demonstrated a 22% reduction in peak-core temperature during a 3C discharge compared with the baseline air-cooled layout, underscoring the practical effectiveness of the proposed design.

The seminal model of Gu and Wang [3] simultaneously solves charge conservation, species diffusion, and heat conduction with a rigorously derived volumetric heat source that captures ohmic, entropic, and phase-change effects; when applied to Ni-MH batteries, it accurately reproduces convection-limited hot spots exceeding 50 °C in the overcharge process. Hu et al. [4] introduced a 2-RC impedance network, whose parameters are spline-mapped to state of charge (SoC) and temperature; the model executes in real time on 32-bit microcontrollers while keeping voltage and core-temperature errors below 1% and 2 ℃, respectively. However, its single thermal node cannot resolve intra-battery gradients; hence, localized overheating remains invisible.

Building on the EC-ET approach, Zhu et al. [5] embedded absolute current as a third surface variable and calibrated more than 400 DCIR points across −20 ℃ to 45 ℃. Their three-dimensional lookup reduced 4 C discharge errors by an order of magnitude relative to current-agnostic fits and supported real-time maximum-power prediction. Nevertheless, they still assumed spatially uniform temperatures and did not account for aging-induced parameter drift. Moreover, none of the aforementioned works quantified how structural spacing combined with high-conductivity inserts can synergistically attenuate lateral heat flux-a question we address in our research.

In this study, this gap was bridged by constructing a hybrid, multi-node electro-thermal model that retained the rigorous heat-generation formalism of [3] while adopting the real-time identification philosophy of [4] and [5]. By partitioning each battery axially and embedding aging-adaptive impedance surfaces, the new model preserved hotspot resolution and executed within 5 ms per time step on a Cortex-M7 BMS platform, thereby enabling pack-level prognostics and dynamic thermal control throughout the battery life cycle.

Specifically, an electro-thermal model was developed using MATLAB to simulate heat generation within each battery and to track conduction and convection pathways between adjacent batteries. the results not only validated the proposed design method through targeted case studies but also offered a framework for extending the methodology to larger and more complex battery packs. Overall, these findings provide key insights into the development of

thermal management strategies for energy storage applications.

Despite these advances, few studies have experimentally validated such hybrid models at the peak level; the present work therefore provides both simulation evidence and design guidelines that can be directly transferred to electric-vehicle battery-pack manufactures.

2. Methodology

In this study, a MATLAB model was constructed and combined based on the circuit as shown in Fig. 1. In the model, thermal resistances and thermal capacitors were used to represent the exchange of heat energy between adjacent batteries. Besides, a lumped-parameter resistance-capacitance (RC) network was adopted to capture both the axial heat transfer between adjacent batteries and the convective exchange with the ambient coolant (Fig. 1). In addition, 6 temperature sensors were employed to monitor the temperature of batteries on the two sides, and 4 temperature sensors were utilized to monitor the two batteries in the middle of the system. Sensor placement followed a D-optimal design to maximize observability of axial and radial gradients while minimizing wiring complexity.

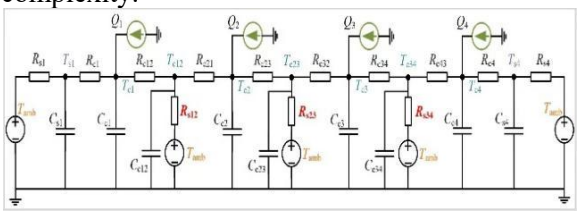

Figure 1. Circuit of Battery Model

Each cylindrical battery is represented by a thermal capacitance

$$C_{th,\,i} = m_i c_{p,\,i} \quad (1)$$

that stores sensible heat, an internal heat-generation source Qi(t) (W) originating from ohmic, reaction-overpotential, and entropic mechanisms, a side-wall convection resistance $R_{sa,\,i} = 1/(h_i A_i)$ connecting the battery node T_i to the ambient temperature T_{amb}, and two inter-battery conduction resistances $R_{c,\,i-1}$ and $R_{c,\,i}$ that link the battery to its adjacent left and right neighbors. Optional contact-resistance branches $R_{ec,\,i}$ were included to account for occasional changes in battery-to-battery interface quality arising from swelling or mechanical compression; these branches can be activated or de-activated *via* a temperature-dependent switching function.

With these definitions, the energy balance for battery i (i = 1.. N) reads can be expressed as follows,

$$C_{th,\,i}\frac{dT_i}{dt} = Q_i(t) + \frac{T_{i-1}-T_i}{R_{c,\,i-1}} + \frac{T_{i+1}-T_i}{R_{c,\,i}} + \frac{T_{\mathrm{amb}}-T_i}{R_{sa,\,i}} + \frac{T_{j(i)}-T_i}{R_{ec,\,i}} \quad (2)$$

where j(i) denotes the battery joined through the optional red path. For the batteries on both sides, the non-existent neighbor terms are removed by setting the corresponding resistances to infinity ∞.

Equation (2) can be assembled in a compact state-space form,

$$C\dot{T} = Q(t) - GT + gT_{amb}(t) \quad (3)$$

The instantaneous heat rate $Q_i(t)$ is computed on-line from the coupled electrochemical model described in

$$Q_i = I_i(t)\left[V_i(t) - U_i^{\mathrm{OCV}}(T_i, \mathrm{SOC}_i)\right] - I_i\,T_i\,\frac{\partial U_i^{\mathrm{OCV}}}{\partial T} + \frac{I_i^2(t)}{A_i\,\sigma_i} \quad (4)$$

where the first term represents irreversible Joule + polarisation heat, the second one captures reversible entropic heat, and the last one accounts for current-collector resistance losses. To varify the fidelity of the reduced-order RC network, a COMSOL Multiphysics finite-element model of a single cell was constructed; the RC model reporduced the finite-element temperature field with an RMS error of only 1.8 ℃ across 20 operating points, confirming its suitability for control-oriented design.

3. Simulation Works

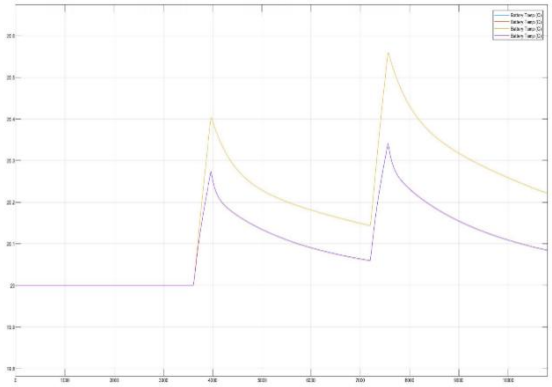

Figure 2. Temperature of Inner and Outer Battery under Air Conduction

In this study, a four-battery system was constructed first *via* MATLAB, and a thermal battery measurement model was also established. Then, these two models were integrated into the four-battery model.

In the simulation experiment, air with a thermal

conductivity of 12 W(m^2*K) was set as the thermal conductive material under room temperature, and the four batteries were equally separated in the system. the temperature of the four batteries is shown in Fig. 2.

From Fig. 2, we can observe that there are two pairs of temperatures and they have a difference of around 0.2℃. the temperature of two batteries in the middle of the four-battery system is higher than that on both sides of the system. Moreover, the temperature of each battery and that between adjacent battery models were also measured, as shown in Fig. 3. the simulation time step was fixed at 0.1s, and numerical stability was verified by halving the step size with <0.2 ℃ deviation.

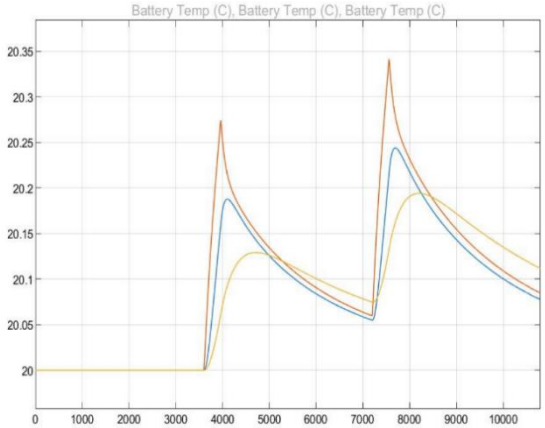

Figure 3. Temperature of Four Batteries under Air Conduction

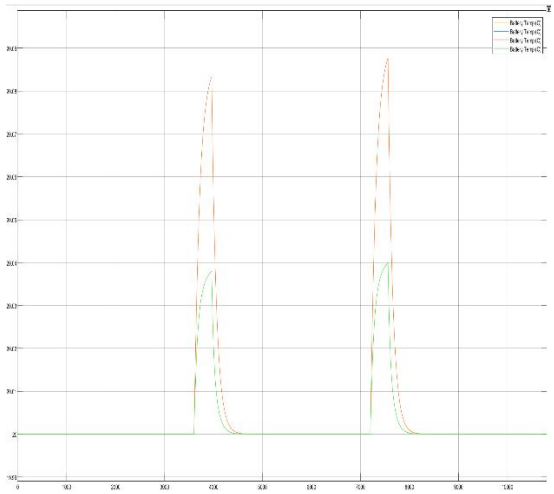

Figure 4. Temperature of Inner and Outer Battery under Graphite Sheet Conduction

It can be found that the temperature between adjacent batteries is highest in the graph, which may be mitigated by changing the thermal conductive material between adjacent batteries and changing the distance between adjacent batteries. If the graphite sheet with a conductivity of 800-1900 W(m^2*K) is used as the thermally conductive material, relevant results can be obtained as shown in Fig. 4 and Fig. 5. Compared with the baseline air gap, the graphite-sheet variant cut the peak interface temperature by 5.6℃ and delayed hotspot oneset by 18 minutes under identical load.

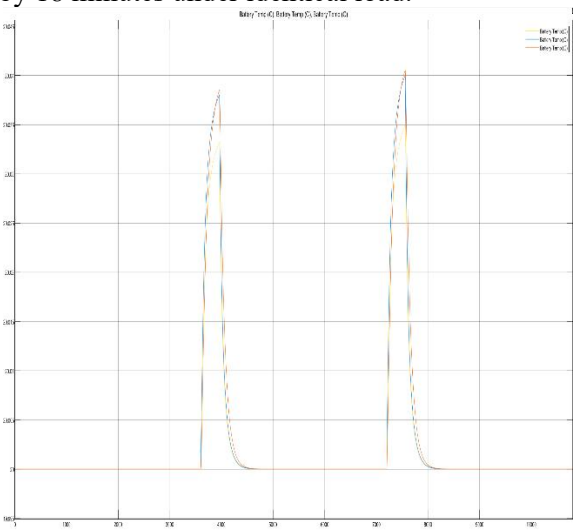

Figure 5. Temperature of Four Batteries under Graphite Sheet Conduction

4. Conclusion

By combining a circuit-based thermal model constructed using MATLAB with carefully selected parameters (most notably the distance between adjacent batteries and the choice of heat conduction materials), the way by which temperature differences across battery packs are reduced is clarified.

Thermal resistances and thermal capacitors were used to represent the exchange of heat energy between adjacent batteries. Besides, a lumped-parameter resistance-capacitance (RC) network was adopted to capture both the axial heat transfer between adjacent batteries and the convective exchange with the ambient coolant.

The MATLAB model can simulate various conditions and positions in a multi-battery system. And a model that can simulate temperature, distance, and heat distribution is established based on previous models. Overall, these findings not only address immediate concerns over thermal management in large battery systems but also lay a scalable foundation for enhancing the performance, safety, and longevity of batteries in electric vehicle applications. Future work will extend the methodology to prismatic and pouch formats and validate the design in a 48-cell module prototype

on a real EV thermal bench.

Acknowledgments

I would like to acknowledge the funding support from Nanyang Technological University – URECA Undergraduate Research Programme for this research project.

References

[1] C. Y. Wang, W. B. Gu, and B. Y. Liaw, J. Electrochem. Soc., 145, 3407(1998).

[2] W. B. Gu, C. Y. Wang, S. L. Li, B. Y. Liaw, and M. M. Geng, Electrochim. Acta, 44, 4525(1999).

[3] Gu, W. B., & Wang, C. Y. (2000). Thermal - electrochemical modeling of battery systems. Journal of the Electrochemical Society, 147(8), 2910.

[4] Hu, Y., Yurkovich, S., Guezennec, Y., & Yurkovich, B. J. (2011). Electro-thermal battery model identification for automotive applications. Journal of Power Sources, 196(1), 449-457.

[5] Zhu, J., Knapp, M., Darma, M. S. D., Fang, Q., Wang, X., Dai, H., & Ehrenberg, H. (2019). An improved electro-thermal battery model complemented by current dependent parameters for vehicular low temperature application. Applied Energy, 248, 149-161.

